Appl. Phys. A (2017) 123:300
DOI 10.1007/s00339-017-0899-0

Applied Physics A
Materials Science & Processing

RAPID COMMUNICATION

Impedance study of undoped, polycrystalline diamond layers obtained by HF CVD

Kazimierz Paprocki[1] · Kazimerz Fabisiak[1,2] · Anna Dychalska[3] · Mirosław Szybowicz[3] · Alina Dudkowiak[3] · Aizhan Iskaliyeva[4]

Received: 9 October 2015 / Accepted: 8 March 2017 / Published online: 3 April 2017

Abstract In this paper, we report results of impedance measurements in polycrystalline diamond films deposited on n-Si using HF CVD method. The temperature was changed from 170 K up to RT and the scan frequency from 42 Hz to 5 MHz. The results of impedance measurement of the real and imaginary parts were presented in the form of a Cole–Cole plot in the complex plane. In the temperatures below RT, the observed impedance response of polycrystalline diamond was in the form of a single semicircular form. In order to interpret the observed response, a double resistor–capacitor parallel circuit model was used which allow for interpretation physical mechanisms responsible for such behavior. The impedance results were correlated with Raman spectroscopy measurements.

1 Introduction

Polycrystalline diamond films have several applications in different industrial areas, because of their high density, hardness, chemical inertness, etc [1]. In the microelectronic industry, these chemical vapor deposited (CVD) films have a great potential as gate dielectric, intermetal dielectric, and passivation layers. These films can be deposited by several techniques, such as Hot Filament Chemical Vapour Deposition (HF CVD), Microwave Plasma CVD (MP CVD), Plasma Jet CVD, or Flame CVD [2].

The film characteristics depend on several different deposition process parameters, such as the gas composition and pressure, the substrate temperature, the energy of the impinging ions, etc [3]. The presence of hydrogen in the gas phase promotes the formation of sp^3 C structures but co-deposition of sp^2 carbon phase, as detected by Raman spectroscopy, also takes place [4].

Due to its superior physical and chemical properties, diamond can be used as an electronic or optoelectronic material because of its high Johnson and Keyes figures of merit values [5]. However, the electrical and optical properties of diamond films strongly depend on the film preparation conditions. Compared with natural diamond, CVD diamond is usually polycrystalline and contains various defects produced during the deposition procedure. Therefore, it is necessary to establish the relationship between the preparation conditions and the structural and electrical properties of diamond films for electronic or optoelectronic applications.

In general, polycrystalline diamond films can be considered as composed from diamond microcrystals oriented in different direction with respect to the substrate surface. The quality of diamond layers increases as the grain size increases starting from the substrate nucleation side to the top of the diamond layer [6].

The larger grains induce a decrease of GB phase in the film what results that diamond layer will have smaller content of the sp^2-hybridized carbon phase.

The sizes of grain boundaries and thus concentration of sp^2 carbon phase eventually can lead to limitations in electronic performances of polycrystalline diamond layers.

✉ Kazimerz Fabisiak
kfab@ukw.edu.pl

1 Institute of Physics, Kazimierz Wielki University, Powstańców Wielkopolskich 2, 85-090 Bydgoszcz, Poland

2 Medical Physics Department, Oncology Center, I. Romanowskiej 2, 85-796 Bydgoszcz, Poland

3 Faculty of Technical Physics, Poznan University of Technology, Piotrowo 3, 60-965 Poznan, Poland

4 Chair of Mathematics and Physics, WKSU, Oral, Kazakhstan 090000

The impedance spectroscopy is a very sensitive technique to study electrical conduction path in polycrystalline materials and allows for better understanding the role of grain surface and GBs on charge transport mechanisms.

In present work, the diamond samples were grown by hot filament HF CVD technique, and frequency dependent admittance was measured as a function of temperature in the 42 Hz–5 MHz frequency range.

The diamond film quality was checked using Scanning Electron Microscopy (SEM), Raman spectroscopy, and X-Ray Diffraction (XRD).

2 Experimental

The diamond films were grown at the rate of 0.2 µm/h on ultrasonically cleaned, monocrystalline n-Si wafers [(10×10) mm, 0.2 mm thickness] as substrates by HF CVD technique. The stainless-steel chamber was water-cooled. The total pressure during growth was 80 mbar. Deposition was carried out using methane as the carbon containing gas, diluted in H_2. The total gas flow rate was fixed at the 100 sccm, and the percentage flows for CH_4 and H_2 were changed from 2.3 to 3 vol%. Prior to growth, the substrates were seeded with 1 µm diamond powder in an ultrasonic bath. The growth temperature was estimated to be ~750 °C, and the thickness of the films are 10.02 and 11.5 µm, respectively. Further details of the deposition system are available from an earlier publication [7].

The Raman spectra were recorded at room temperature in back scattering geometry using Renishaw in Via Raman spectrometer. A tunable Ar ion laser was used for 488 nm as an excitation source. The Raman scattering spectra were investigated in the spectral range of 1000–2000 cm^{-1}. All data collection were analyzed using Renishaw WiRE 3.1 software using curve fitting method.

X-ray diffraction patterns were recorded at room temperature by DRON-4a, Θ-2Θ XRD diffractometer using a Cu Kα X-ray source.

The impedance measurements were recorded in frequency range of 42 Hz to 5 MHz using HIOKI 3532-50 LCR HiTester. The measurements were performed in temperature range of 167–300 K in N_2 atmosphere and with electrode configuration as shown in Fig. 1.

The results analysis was performed using homemade software and EIS Spectrum Analyser program [8].

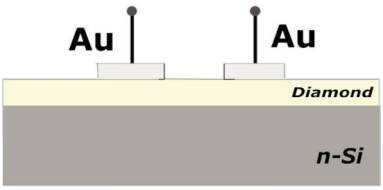

Fig. 1 Electrode system used in the ac-measurements

3 Results and discussion

The Fig. 2 presents the morphology of diamond film deposited at the same reaction pressure of 80 mbar. The surface morphology of the investigated diamond films was found to depend on the concentration of methane vapor in the working gas. With increasing methane, concentration from 2.3 to 3% did not change drastically.

The changes in diamond film qualities are clearly seen in their Raman spectra presented in Fig. 3.

The diamond Raman lines for both samples are peaked at about 1331.6 cm^{-1} which is very close to the value of 1332.5 cm^{-1}, characteristic for diamond monocrystal [9]. The diamond Raman lines are presented in (Fig. 3).The both spectra are characterized, except sharp diamond at around 1331.6 cm^{-1}, by broad luminescence background, with different slopes m, and G-band at around 1530 cm^{-1}, better pronounced in the sample deposited at higher methane concentration.

The broad luminescence background (see Fig. 3) may arise from hydrogen in amorphous a-C:H carbon being admixture of CVD diamond layer. The slope m of luminescence background is proportional to hydrogen

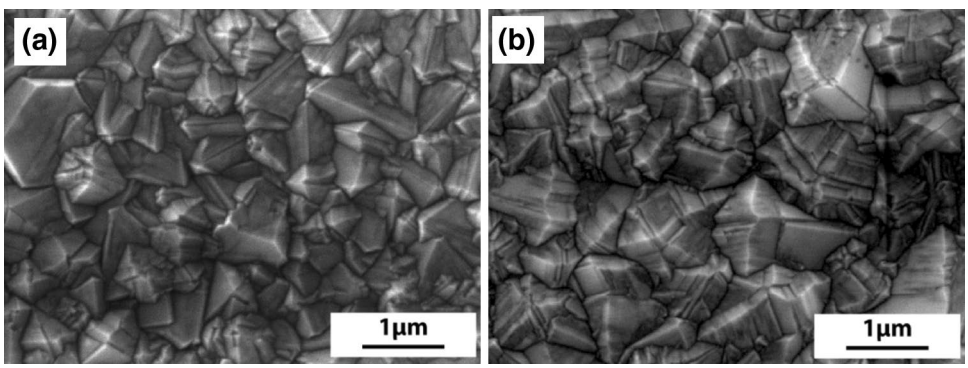

Fig. 2 SEM picture of diamond layers deposited at methane concentrations of : **a** 3.0% and **b** 2.3%

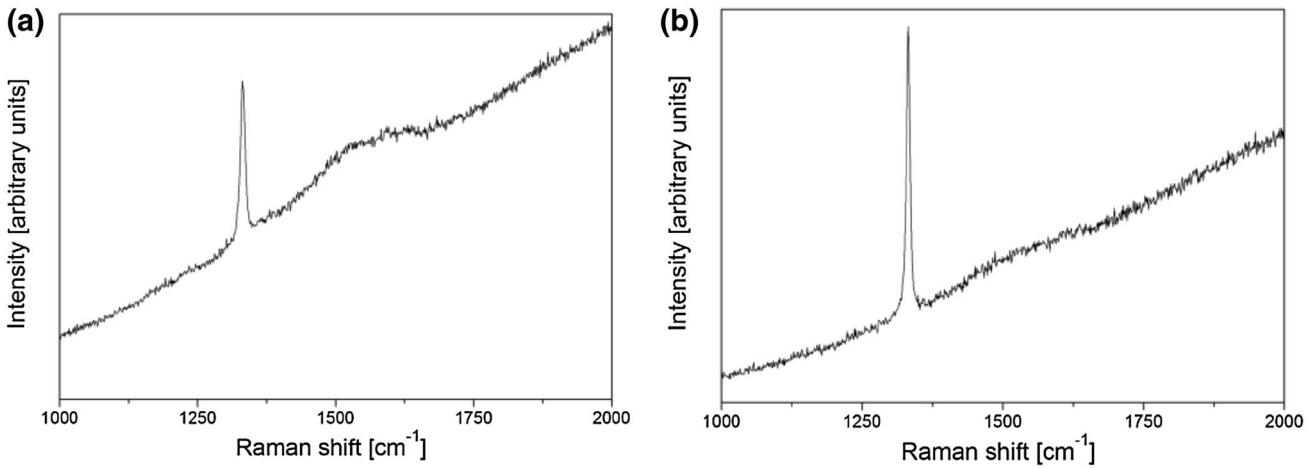

Fig. 3 Raman spectra of the diamond films presented in Fig. 2

concentration in CVD diamond film [10]. Because of higher slope m, the samples are characterized by higher hydrogen content which is mainly associated with existence of sp^2 carbon phase admixture which was also confirmed by earlier observation [11–15]. The influence of methane concentration on diamond quality is shown in Table 1.

The sp^2/sp^3 ratio was calculated using procedure described in our earlier paper [3], and residual stress was calculated from the shift of diamond Raman peak from its 1332.5 cm^{-1} ideal position using formula proposed by Ralchenko et al. [16]. The calculated residual stresses in both samples have very similar values of about 0.2 GPa.

The average grain sizes were estimated on basis of X-ray diffraction measurements using Debye–Scherrer equation [3, 17]. The crystallites preferred orientation in the layers can be quantitatively evaluated using texture coefficient, $T_{C(hkl)}$ [17, 18]. The diffraction spectra of the studied diamond layers, together with texture coefficients, are presented in Fig. 4.

The differences between samples are not detected by SEM but are clearly seen in X-ray diffraction and Raman spectroscopy measurements.

The most pronounced differences between presented diamond layers are seen in the values of their preferred orientations (see Fig. 4). Additionally, the layer deposited at higher methane concentration is characterized by higher value of Full Width at Half Maximum (FWHM) which is an indication of diamond quality. The decrease of diamond layer quality may be caused by higher concentration of sp^2 (higher value of sp^2/sp^3 ratio)-hybridized carbon phase which leads to higher slope of the luminescence background.

3.1 Impedance spectroscopy

The electrical conduction path in polycrystalline diamond films can be realized by grain boundaries, grain interiors, and amorphous carbon phase admixture situated mainly on grain boundaries. The details of Impedance Spectroscopy can be found elsewhere [19]. This techniques allows to propose equivalent circuit for studied materials which give possibility to compare the experimental data with simulated data by changing the parameters of the equivalent circuit.

The obtained results show that for the conduction paths in polycrystalline diamond films the both grain boundaries and grain interior are responsible as well.

As it is seen in Fig. 5, a Coole–Coole plots have a single semicircular shape at all studied temperatures. The diameter of the semicircular signal is decreasing with increasing temperature. For theoretical simulation, two parallel RC circuits, describing contribution to electrical conduction of diamond films from both grain interior and grain boundaries, in series were used.

Table 1 Quality parameters of the studied diamond layers

	Pressure (mbar)	CH_3OH/H_2 (%)	Average grain sizes (μm)	The thickness of layers (μm)	sp^2/sp^3 ratio (%)	FWHM (cm^{-1})	slope (cm)
DPK25 (a)	80	3.00	0.58	11.50	24.22	9.4	9.98
DPK26 (b)	80	2.30	0.73	10.02	9.43	7.8	3.71

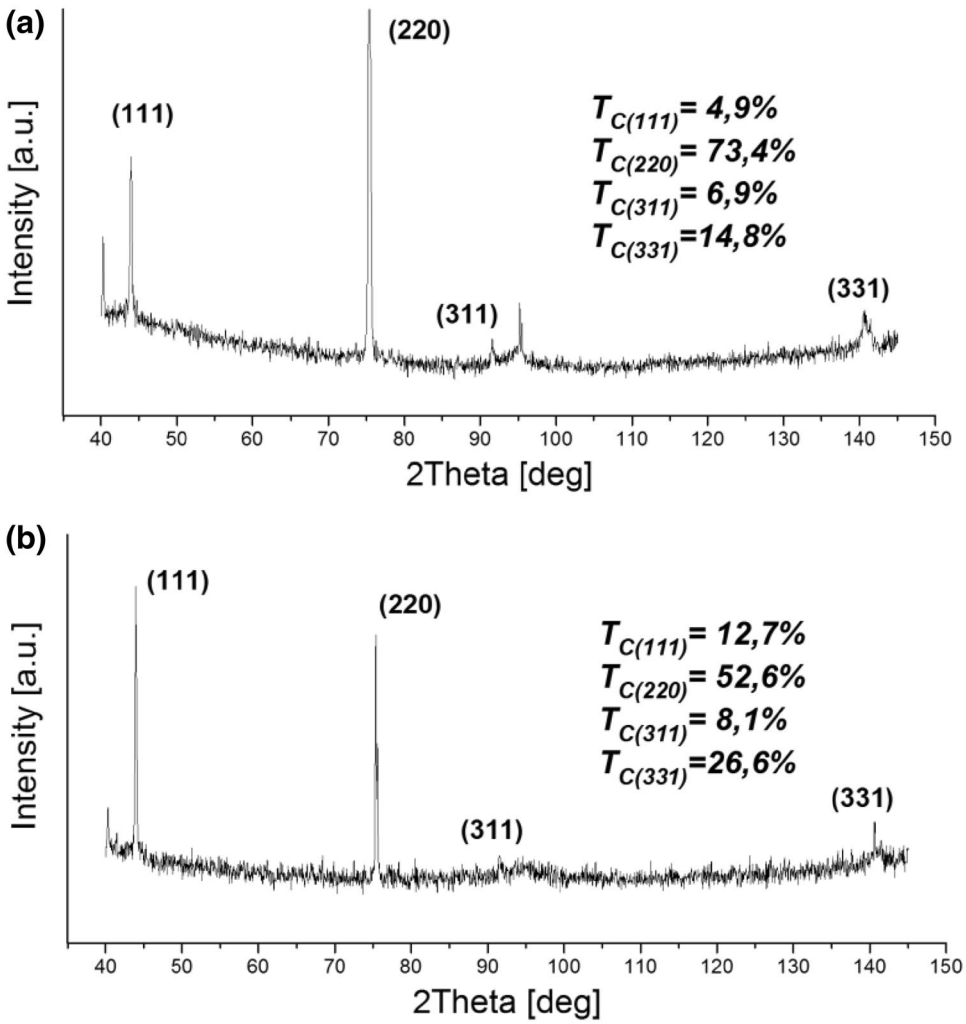

Fig. 4 The XRD spectra of the diamond layers shown in Fig. 2

The used fitting procedure was similar as that described by Kleitz and Kennedy [20] and allows the determination of resistance and capacitance with a very good precision.

The symbols R_{gi}, R_{gb}, C_{gi}, and C_{gb} are resistance and capacitance of grain interior (gi) and grain boundaries (gb), respectively. The resistor represents electronic conduction mechanisms, and capacitor is responsible for the diamond polarizability.

As it shown in Fig. 5, both samples show similar temperature dependence impedance characteristics.

The performed simulation, using EIS software, showed that temperature dependent is only one resistor, i.e., R_{gi}, while both capacitors did not change with temperature and are equal: $C_{gi} \sim 1.5 \times 10^{-9}$ F, $C_{gb} \sim 1.8 \times 10^{-10}$ F for sample Dkp25 and $C_{gi} \sim 1.6 \times 10^{-10}$ F, $C_{gb} \sim 1.4 \times 10^{-9}$ F for sample Dpk26. The second resistors R_{gb} were very weakly temperature dependent and have average values of 400 and 1450 Ω for Dpk25 and Dpk26 samples, respectively.

Our results are in good agreement with those obtained by Ye et. al [21]. According to their work, the contribution to impedance from grain boundaries becomes significant at higher temperatures even above 250 °C.

The dependence of R_{gi} versus temperature for both samples is shown in Fig. 6.

Such behavior seems to be understandable because the structure of grain bound should not change with temperature, while conduction mechanism inside grain should be thermally activated because hydrogenated diamond shows semiconducting properties [12]. However, for Dpk26 sample at even lower temperatures are visible both mechanisms (two overlapping semicircles) which may be associated with an preferential orientation of diamond microcrystal (see texture coefficients in Fig. 4) and with an inhomogeneous spatial distribution of sp^2 carbon in diamond layers. It is known that the most defective diamond crystal planes are (111) planes [6, 22]. The differences in preferred orientations ($T_{C(hkl)}$ shown in Fig. 4) in both diamond layers may have an influence on conduction mechanisms.

As it is seen from Fig. 6, both samples show slightly different slopes of the plot $\log(R_{gi})$ versus $1/T$, which can be

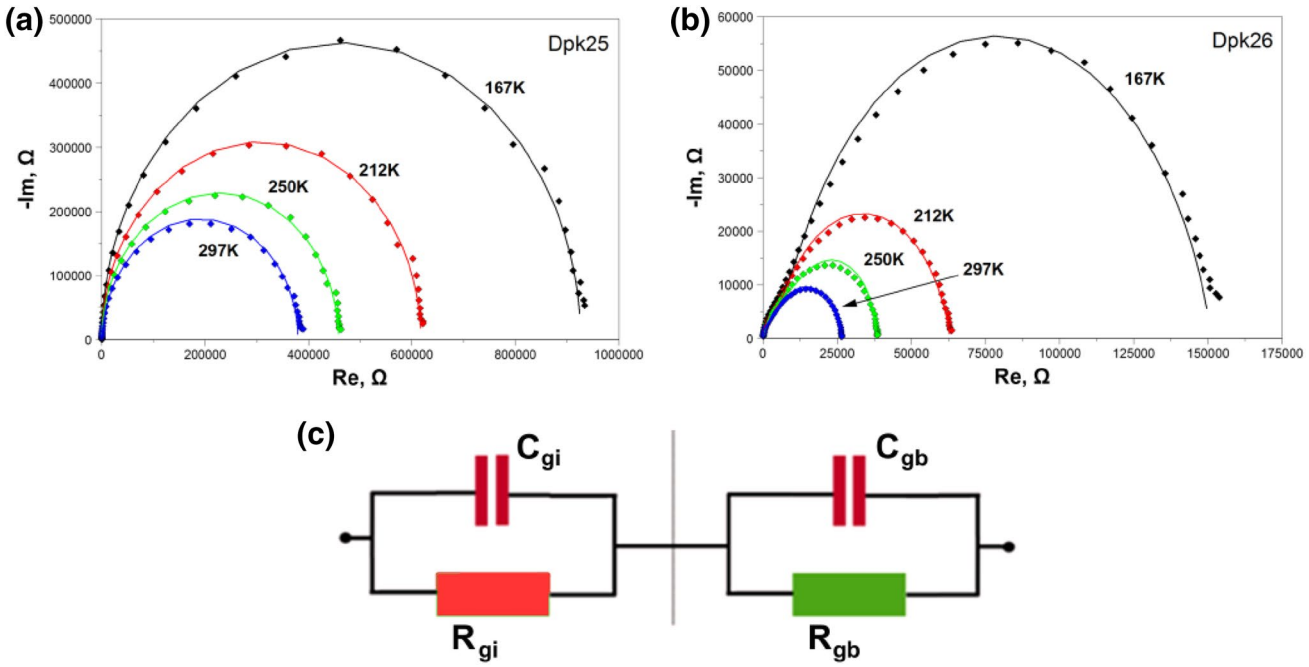

Fig. 5 Coole–Coole plots: **a, b** (*filled square* exp. *curve line* theor.) and equivalent circuit (**c**)

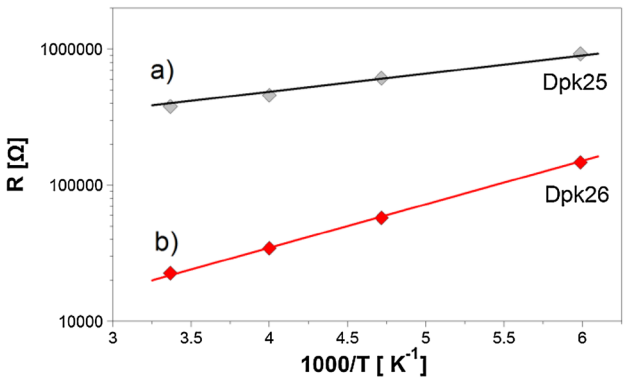

Fig. 6 The temperature dependence of grain interior (R_{gi}) resistances for the studied diamond layers

caused by different hydrogen concentrations, as it is indicated by the slope *m* of the corresponding Raman spectra.

4 Conclusions

For synthesis of diamond films, the hot filament CVD method was used. The obtained layers have been characterized using SEM, XRD, Raman spectroscopy, and impedance spectroscopy. The impedance measurement were performed in the temperature range of 160–290 K and have been presented in the form of a Cole–Cole plot. The grain interior and grain boundary contributions to the electrical mechanisms were identified. It was found that only grain interior electrical conduction has thermally activated character. As it is seen from Fig. 6, the activation energy can be dependent on hydrogen content in diamond films. More detailed investigations for much broader temperature range may help more directly explain the suggested mechanisms.

References

1. K.E. Spear, J.P. Dismuckes, Synthesis diamond: emerging CVD science and technology. (Wiley, New York, 1994)
2. J.J. Gracio et al., J. Phys. D: Appl. Phys **43**(37), 374017 (2010)
3. K. Fabisiak, et al., Mater. Sci. Eng. B **177**(15), 1352 (2012).
4. K. Fabisiak et al., Cryst. Res. Technol. **45**(2), 167 (2010)
5. J. Edgar, J. Mater. Res. **7**(1), 235 (1992)
6. K. Fabisiak et al., Opt. Mater. **30**(5), 763 (2008)
7. K. Fabisiak et al., Opt. Mater. **28**(1–2), 106 (2006)
8. A.S. Bandarenko, G.A. Ragoisha, in *Progress in Chemometrics Research*, ed. by A.L. Pomerantsev (Nova Science Publishers, New York, 2005), p. 89
9. S. Solin, A. Ramdas, Phys. Rev. B **1**(4), 1687 (1970)
10. G. Adamopoulos et al., J. Appl. Phys. **96**(11), 6348 (2004)
11. D. Ballutaud, et al., Diamond Relat. Mater. **17**(4–5), 451 (2008).
12. S. Michaelson et al., J. Appl. Phys. **102**(11), 113516 (2007)

13. R. Ramamurti et al., J. Vac. Sci. Technol. A **24**(2), 179 (2006)
14. S. Linnik, et al., Mater. Today: Proc. 3, S138 (2016).
15. J.A. Bennett et al., J. Electrochem. Soc **151**(9), E306 (2004)
16. V.G. Ralchenko, et al., Diamond Relat. Mater. **4**(5–6), 754 (1995).
17. D.I. Rusu, et al., Acta Phys. Pol. A **119**(6), 850 (2011).
18. C.T. Kuo et al., Thin Solid Films **290–291**, 254 (1996)
19. J.R. Macdonald, W.B. Johnson, *Impedance Spectroscopy* (Wiley, New York, 2005), p. 1
20. J.H. Kennedy et al., Electrochim. Acta **24**(7), 781 (1979)
21. H. Ye et al., J. Appl. Phys **94**(12), 7878 (2003)
22. J.E. Butler, I. Oleynik, Philos. Trans. R. Soc. Lond. A **366**(1863), 295 (2008).